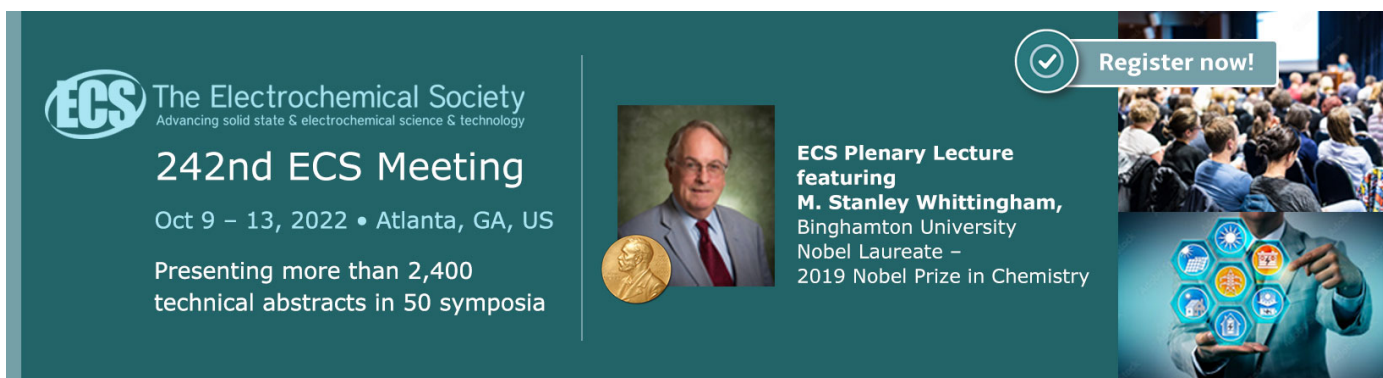


OPEN ACCESS

## Thermodynamic Design of Electrolyte for CuO/Cu<sub>2</sub>O Bilayer by Anodic Electrodeposition

To cite this article: Ryutaro Miura *et al* 2021 *J. Electrochem. Soc.* **168** 062506

View the [article online](#) for updates and enhancements.




 The Electrochemical Society  
Advancing solid state & electrochemical science & technology

**242nd ECS Meeting**  
Oct 9 – 13, 2022 • Atlanta, GA, US  
Presenting more than 2,400  
technical abstracts in 50 symposia


**ECS Plenary Lecture**  
featuring  
**M. Stanley Whittingham,**  
Binghamton University  
Nobel Laureate –  
2019 Nobel Prize in Chemistry

 Register now!





# Thermodynamic Design of Electrolyte for CuO/Cu<sub>2</sub>O Bilayer by Anodic Electrodeposition

Ryutarō Miura, Atsushi Kitada,<sup>1b</sup> Kazuhiro Fukami,<sup>\* 1b</sup> and Kuniaki Murase<sup>\*,z 1b</sup>

Department of Materials Science and Engineering, Kyoto University, Japan

Electrodeposition of multilayered semiconductors requires a bath design to electrodeposit the upper layer(s) without dissolving the base layer(s) below. We present herein a reliable approach to bath design based on thermodynamics from the viewpoint of complexation with ligands. A CuO/Cu<sub>2</sub>O bilayer film was targeted as an example. We searched a thermodynamic database of complexation constants for ligands that could form a complex with Cu(II) but not with Cu(I), and identified monoethanolamine as one of the best candidates. Using a Cu(II)-monoethanolamine alkaline aqueous bath, we experimentally confirmed that a CuO upper layer could be deposited without dissolving the Cu<sub>2</sub>O base layer. We believe that this design is applicable to other bilayer films produced by electrochemical techniques.

© 2021 The Author(s). Published on behalf of The Electrochemical Society by IOP Publishing Limited. This is an open access article distributed under the terms of the Creative Commons Attribution 4.0 License (CC BY, <http://creativecommons.org/licenses/by/4.0/>), which permits unrestricted reuse of the work in any medium, provided the original work is properly cited. [DOI: 10.1149/1945-7111/ac064c]



Manuscript submitted March 11, 2021; revised manuscript received May 11, 2021. Published June 9, 2021. *This was paper 1428 presented during PRiME 2020, October 4–9, 2020.*

Supplementary material for this article is available [online](#)

Multilayered semiconductors have been widely studied for various applications, including p-n junction diodes,<sup>1,2</sup> p-n junction solar cells,<sup>3,4</sup> and photoelectrodes.<sup>5,6</sup> Vapor deposition,<sup>7,8</sup> chemical solution deposition,<sup>9,10</sup> and electrodeposition<sup>11,12</sup> techniques have been proposed for the fabrication of multilayered semiconductors. Among these, electrodeposition from aqueous solutions has many advantages, including low temperature, low cost, and ease of large-scale deposition.

In general, to electrodeposit multilayered semiconductors, different electrodeposition solutions are employed for each layer. Therefore, in any system, there is a potential drawback of the base layer(s) being attacked by the solution for the layer(s) above. Each solution must therefore be designed such that the solution for upper layer(s) would not damage the layer(s) below. For example, it is not workable if the base layer(s) spontaneously dissolves, or corrodes, in the solution designed for a subsequent layer. Careful selection of the components and conditions of the electrodeposition solution for the upper layer, e.g., ligands for metal ions and pH, is required. Thermodynamic data, such as complexation constants, are useful in this process. If the ligands in the solution for the upper layer can form complexes with the metal ion of the base layer, the surface of the base layer will dissolve. Such partial dissolution may result in uneven layer thickness and incorporation of impurities from the solution, affecting the reproducibility and performance of the multilayers.

In this paper, we focused on a CuO/Cu<sub>2</sub>O (CuO on top of Cu<sub>2</sub>O) bilayer. This bilayer may be employed as the photocathode in a water splitting system for hydrogen evolution.<sup>13,14</sup> Preparation of the CuO/Cu<sub>2</sub>O layers by electrodeposition requires fine pH control and control of the complexation of copper cations with different valences, making it more difficult than some other systems. If the CuO/Cu<sub>2</sub>O bilayer can be fabricated using the strategy proposed in this study, the method may be applicable not only to other semiconductors, but also to bilayers of metals and alloys.

To fabricate CuO/Cu<sub>2</sub>O layers by electrodeposition, it is necessary to design CuO electrodeposition solutions that do not attack the Cu<sub>2</sub>O layer underneath. A conventional method for CuO electrodeposition is to use an ammoniacal solution.<sup>15</sup> This method employs electrochemically-induced chemical deposition (EICD), in which CuO is deposited by an acid-base reaction using a local pH drop caused by oxygen evolution under anodic overpotentials. This is not

strictly an electrodeposition, but in this paper, this type of CuO deposition is referred to as anodic CuO electrodeposition. Previous studies of anodic CuO electrodeposition did not consider whether the Cu<sub>2</sub>O base layer was affected by the CuO electrodeposition solution, especially from the viewpoint of thermodynamics or stability constants of ligands and Cu(II) or Cu(I) ions. As described below, the CuO electrodeposition solution proposed by Izaki et al. using an ammoniacal solution is not suitable for forming CuO on Cu<sub>2</sub>O.<sup>15</sup> In this study, we present a solution design for a CuO/Cu<sub>2</sub>O bilayer through a thermodynamic database search and experimental proof, and successfully achieved anodic electrodeposition of the CuO upper layer without dissolving the Cu<sub>2</sub>O base layer.

## Experimental

**Screening ligands in a database.**—Using a thermodynamic database,<sup>16–18</sup> we searched for ligands that do not readily form complexes with monovalent copper cation, easily form complexes with divalent copper cation, and are relatively inexpensive and versatile. When there was no entry for the complex formation constant with Cu(I), it was assumed that a ligand did not form a complex with Cu(I).

**Preparation of anodic CuO electrodeposition solutions and immersion test of Cu<sub>2</sub>O.**—All aqueous solutions were prepared with reagent grade chemicals purchased from Nacalai Tesque and deionized 18 MΩ water obtained using the Milli-Q system. Monoethanolamine (MEA; 2-aminoethanol-1-ol, 2-aminoethanol)-based Cu(II) solution consisted of 0.05 M (M = mol l<sup>-1</sup>) copper(II) sulfate pentahydrate (CuSO<sub>4</sub>·5H<sub>2</sub>O) and 0.125 M MEA at pH = 12.5 adjusted with NaOH. Tris(hydroxymethyl)aminomethane (Tris)-based Cu(II) solution consisted of 0.05 M CuSO<sub>4</sub>·5H<sub>2</sub>O and 0.1 M Tris at pH = 12.5 adjusted with NaOH. Trimethylenediamine (TMDA)-based Cu(II) solution consisted of 0.05 M CuSO<sub>4</sub>·5H<sub>2</sub>O and 0.1 M TMDA at pH = 7.4 adjusted with H<sub>2</sub>SO<sub>4</sub>. Ammoniacal Cu(II) solution consisted of 0.05 M copper(II) nitrate trihydrate (Cu(NO<sub>3</sub>)<sub>2</sub>·3H<sub>2</sub>O) and 0.1 M ammonium nitrate (NH<sub>4</sub>NO<sub>3</sub>) at pH = 9 adjusted with aqueous NH<sub>3</sub>, referring to previous research on CuO electrodeposition.<sup>15</sup> This ammoniacal solution was used for comparison with MEA solution.

To verify whether Cu<sub>2</sub>O was stable and would not dissolve in the MEA-based solution or in the ammoniacal solution, Cu<sub>2</sub>O immersion tests were performed for 5 h after degassing for 30 min. Nitrogen deaeration was performed to eliminate dissolved oxygen. The weight of each sample before and after the immersion test was measured using a microbalance (XP6, Mettler Toledo Ltd.), to confirm the stability of Cu<sub>2</sub>O.

\*Electrochemical Society Member.

<sup>z</sup>E-mail: [murase.kuniaki.2n@kyoto-u.ac.jp](mailto:murase.kuniaki.2n@kyoto-u.ac.jp)

**Cathodic electrodeposition of Cu<sub>2</sub>O layers.**—Cu<sub>2</sub>O layer preparation was conducted using the traditional method with lactate-based alkaline solution.<sup>19–21</sup> The solution for the Cu<sub>2</sub>O electrodeposition contained 0.4 M copper acetate monohydrate (Cu(CH<sub>3</sub>COO)<sub>2</sub>·H<sub>2</sub>O) and 3.0 M lactic acid (CH<sub>3</sub>CH(OH)COOH). The pH of the solution was adjusted to 12.5 with NaOH. The electrodeposition was carried out in a three-electrode cell. Conductive fluorine-doped tin oxide (FTO) glass was used as the substrate, i.e., the working electrode, for the deposition. Pt sheet was used as the counter electrode, and an Ag/AgCl electrode in 3.33 M KCl was used as the reference electrode. Before electrodeposition, the FTO glass was washed ultrasonically in acetone for 5 min and in ethanol for 5 min, and then electrolytically degreased at 10 mA cm<sup>-2</sup> in 1 M NaOH aq. The Cu<sub>2</sub>O electrodeposition was performed potentiostatically at -0.4 V vs Ag/AgCl at 313 K. The total electric charge was 1.5 C cm<sup>-2</sup>, which corresponded to a Cu<sub>2</sub>O thickness of about 2 μm.

**Anodic electrodeposition of CuO on Cu<sub>2</sub>O layers.**—The solution for anodic CuO electrodeposition was prepared as described above. Electrochemical experiments were performed in a three-electrode cell similar to that used for Cu<sub>2</sub>O electrodeposition. The above-mentioned Cu<sub>2</sub>O-electrodeposited FTO glass was used as the working electrode. The counter electrode was Pt sheet, and Ag/AgCl electrode in 3.33 M KCl was used as the reference electrode. Cyclic voltammetry (CV) was measured to investigate the behavior of CuO electrodeposition on Cu<sub>2</sub>O. The anodic CuO electrodeposition was carried out potentiostatically and the total electric charge was 1.5 C cm<sup>-2</sup>. Table I summarizes the applied potential and the temperature of each aqueous solution. The electrodeposition potential was determined based on the results of the CV described below. In the case of the ammoniacal solution, the conditions were the same as those in Ref. 15.

**Characterization of CuO/Cu<sub>2</sub>O layers.**—The surface and cross-sectional morphology of the layers were observed using a field-emission scanning electron microscope (FE-SEM; Hitachi Ltd.). X-ray diffraction (XRD) measurements were performed using a Rigaku RINT2000 system with Cu-Kα radiation at 40 kV and 30 mA. X-ray photoelectron spectroscopy (XPS) measurement was performed using a JEOL JPS-9010TRX with monochromatic Al-Kα. UV-vis absorption spectroscopy was performed using a UV-vis self-recording spectrophotometer with an integral sphere (U-3500, Hitachi).

## Results and Discussion

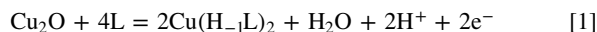
**Determination of appropriate ligands for anodic CuO electrodeposition without Cu(I) complex formation.**—For anodic CuO electrodeposition, it is necessary for the stable pH region of CuO to be at a lower pH than that of the complex of Cu(II). Some ligands that satisfied this condition, i.e., ammonia (NH<sub>3</sub>), mono-ethanolamine (MEA), tris(hydroxymethyl)aminomethane (Tris), and trimethylenediamine (TMDA), were selected; their complexation constants with Cu(II) and Cu(I) are shown in Table II. Figures 1a–1e show pH-speciation diagrams of the complexes calculated using a numeric computing environment, Maple 2019 (Maplesoft). For example, in the case of ammonia, the stable region of CuO exists at lower pH than the stable region of CuL<sub>4</sub><sup>2+</sup>. This indicates that CuO deposition may be performed by utilizing the local pH drop due to

anodic oxygen generation.<sup>15</sup> However, based on the reported stability constants of NH<sub>3</sub> complexes with Cu(I),<sup>22</sup> there is no Cu<sub>2</sub>O-stable region in the pH region where CuL<sub>4</sub><sup>2+</sup> can be present, as shown in Figs. 1a and 1b, and thus Cu<sub>2</sub>O is expected to dissolve. Therefore, Cu<sub>2</sub>O is not suitable as a base layer in this case. In contrast, the other three ligands (MEA, TMDA, and Tris shown in Figs. 1c–1e) do not have reported complexation constants with Cu (I). We thus assumed that they do not form complexes with Cu(I) cation, and considered MEA, TMDA, and Tris to be candidates for anodic CuO electrodeposition on Cu<sub>2</sub>O.

**Investigation of MEA, Tris and TMDA-based solution and immersion test of Cu<sub>2</sub>O for anodic CuO electrodeposition.**—In the solution with [Cu(II)] = 0.05 M and [MEA] = 0.125 M, a precipitate of hydroxide was formed at pH 8.5 as shown in Fig. 1f. When the pH was increased, a deep blue solution without any precipitates was obtained as shown in Fig. 1f; the pH of the resulting solution was 12.5. Similarly, for TMDA and Tris solutions, hydroxide precipitation was observed at low pH as shown in Figs. S1a, S1b (available online at [stacks.iop.org/JES/168/062506/mmedia](https://stacks.iop.org/JES/168/062506/mmedia)), but at high pH, the solution was deep blue without precipitation. These suggested that anodic CuO electrodeposition using a local pH decrease was likely to succeed.

A set of Cu<sub>2</sub>O immersion tests was performed, to ascertain whether Cu<sub>2</sub>O could exist stably in the solutions. The weight changes before and after immersion are summarized in Table III. Weight changes of 320 μg, 10 μg, 10 μg, and 30 μg were observed in the NH<sub>3</sub>, MEA, Tris, and TMDA solutions, respectively. Assuming that the changes were due entirely to the dissolution of Cu<sub>2</sub>O, they corresponded to dissolved thicknesses of Cu<sub>2</sub>O of about 640 nm, 20 nm, 20 nm, 60 nm, respectively. As shown in Figs. 2 and Figs. S1c, S1d, the surface morphology slightly changed after immersion in the MEA, Tris, and TMDA solution, whereas that significantly changed after immersion in the NH<sub>3</sub> solution. These indicated that Cu<sub>2</sub>O is more stable in MEA, Tris, and TMDA solution than in NH<sub>3</sub> solution, and that MEA, Tris, and TMDA solution is more suitable for anodic CuO electrodeposition. Especially among them MEA is most useful ligand because it is relatively inexpensive compared to TMDA and Tris. Therefore, we have investigated the electrodeposition behavior of CuO on Cu<sub>2</sub>O in more detail using the MEA-based solution. However, we describe some results of anodic CuO electrodeposition on Cu<sub>2</sub>O using Tris, TMDA, and NH<sub>3</sub> based solutions briefly in subsequent section.

**CuO electrodeposition on Cu<sub>2</sub>O using MEA-based solution.**—Figure 3 shows cyclic voltammograms for the Cu<sub>2</sub>O-deposited FTO glass (“the Cu<sub>2</sub>O/FTO layer”) in the solution for CuO electrodeposition. In the 1st cycle only, an oxidation wave was clearly observed between open circuit potential (OCP) -0.13 V and +0.2 V. The potential of oxygen evolution at pH 12.5 was calculated to be about +0.285 V vs Ag/AgCl in 3.33 M KCl. Therefore, the oxidation wave corresponded to anodic dissolution of Cu<sub>2</sub>O as expressed in Eq. 1.



(Note that H<sub>-1</sub>L<sup>2-</sup> ion is deprotonated MEA)

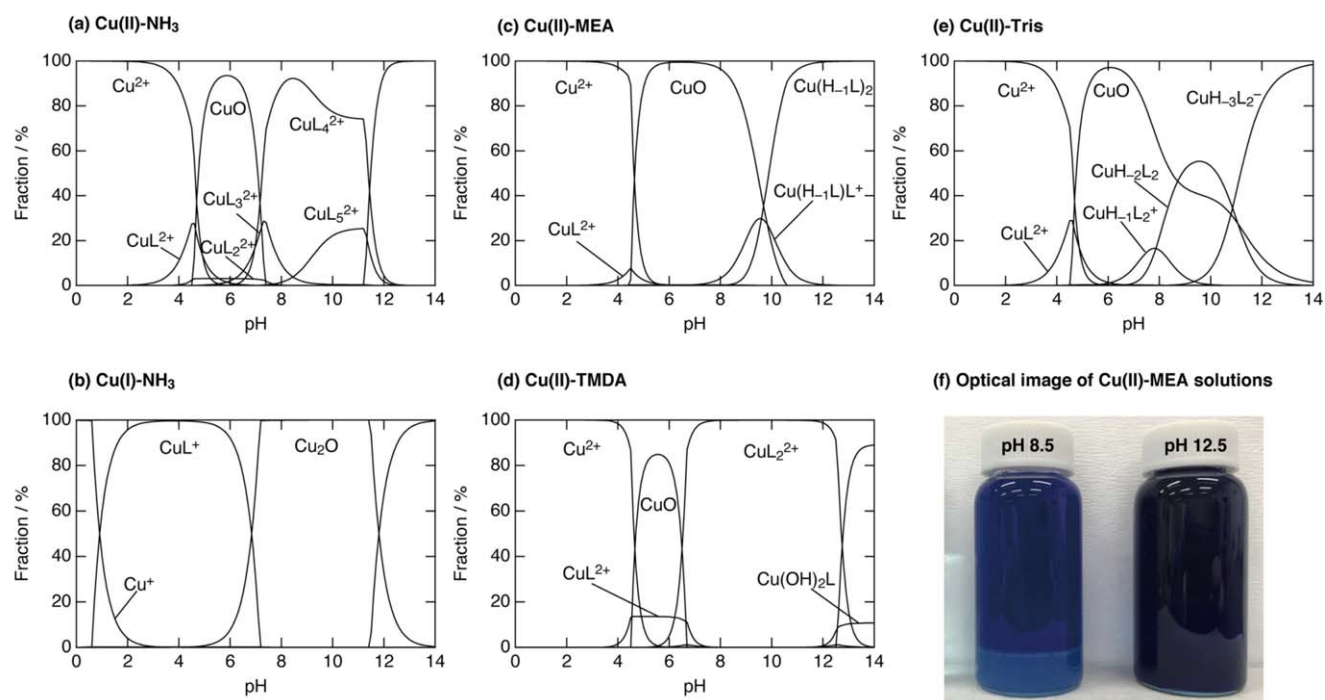
The oxidation wave above +0.4 V was caused by oxygen evolution (Eq. 2).

**Table I. Applied potential and solution temperature during anodic CuO electrodeposition in each ligand solution.**

Ligand	Applied potential (vs Ag/AgCl in 3.33 M KCl)	Solution temperature
MEA	0.45 V	323 K
Tris	0.45 V	323 K
TMDA	0.9 V	363 K
NH <sub>3</sub>	0.9 V	298 K

**Table II.** Stability constants of species containing Cu(II) and L (L = ammonia, mono-ethanolamine, trimethylenediamine, tris(hydroxymethyl)aminomethane) at certain ionic strengths *I*.

	Reaction	LogK	References
NH <sub>3</sub> ( <i>I</i> = 0.5)	H <sup>+</sup> + L = HL <sup>+</sup>	9.32	22
	Cu <sup>2+</sup> + L = CuL <sup>2+</sup>	4.24	
	Cu <sup>2+</sup> + 2L = CuL <sub>2</sub> <sup>2+</sup>	7.83	
	Cu <sup>2+</sup> + 3L = CuL <sub>3</sub> <sup>2+</sup>	10.80	
	Cu <sup>2+</sup> + 4L = CuL <sub>4</sub> <sup>2+</sup>	13.00	
	Cu <sup>2+</sup> + 5L = CuL <sub>5</sub> <sup>2+</sup>	12.43	
	Cu <sup>+</sup> + L = CuL <sup>+</sup>	5.93	
	Cu <sup>+</sup> + 2L = CuL <sub>2</sub> <sup>+</sup>	10.58	
MEA ( <i>I</i> = 1.0)	H <sup>+</sup> + L = HL <sup>+</sup>	9.66	17
	Cu <sup>2+</sup> + L = CuL <sup>2+</sup>	4.4	
	Cu <sup>2+</sup> + 2L = CuL <sub>2</sub> <sup>2+</sup>	8.4	
	Cu <sup>2+</sup> + 2L = Cu(H <sub>1</sub> L)L <sup>+</sup> + H <sup>+</sup>	1.5	
	Cu <sup>2+</sup> + 2L = Cu(H <sub>1</sub> L) <sub>2</sub> + 2H <sup>+</sup>	-8.1	
TMDA ( <i>I</i> = 0.1)	H <sup>+</sup> + L = HL <sup>+</sup>	10.52	23
	2H <sup>+</sup> + L = H <sub>2</sub> L <sup>+</sup>	8.74	
	Cu <sup>2+</sup> + L = CuL <sup>2+</sup>	9.75	
	Cu <sup>2+</sup> + 2L = CuL <sub>2</sub> <sup>2+</sup>	16.9	
	2(CuOHL) = (CuOHL) <sub>2</sub>	2.41	
	CuOHL + H <sup>+</sup> = CuL <sup>2+</sup>	7.66	
	Cu(OH) <sub>2</sub> L + 2H <sup>+</sup> = CuL <sup>2+</sup>	19.36	
Tris ( <i>I</i> = 0.1)	H <sup>+</sup> + L = HL <sup>+</sup>	8.19	18
	Cu <sup>2+</sup> + L = CuL <sup>2+</sup>	4.37	
	Cu <sup>2+</sup> + L = CuH <sub>1</sub> L <sup>+</sup> + H <sup>+</sup>	-2.22	
	Cu <sup>2+</sup> + L = CuH <sub>2</sub> L + 2H <sup>+</sup>	-10.51	
	Cu <sup>2+</sup> + 2L = CuH <sub>1</sub> L <sub>2</sub> <sup>+</sup> + H <sup>+</sup>	1.47	
	Cu <sup>2+</sup> + 2L = CuH <sub>2</sub> L <sub>2</sub> + 2H <sup>+</sup>	-6.39	
	Cu <sup>2+</sup> + 2L = CuH <sub>3</sub> L <sub>2</sub> <sup>-</sup> + 3H <sup>+</sup>	-17.24	
	2Cu <sup>2+</sup> + 2L = Cu <sub>2</sub> H <sub>2</sub> L <sub>2</sub> <sup>2+</sup> + 2H <sup>+</sup>	-1.67	
	2Cu <sup>2+</sup> + 2L = Cu <sub>2</sub> H <sub>3</sub> L <sub>2</sub> <sup>+</sup> + 3H <sup>+</sup>	-9.05	
	Cu <sup>2+</sup> + H <sub>2</sub> O = CuO + 2H <sup>+</sup>	-7.65	
Cu <sup>+</sup> + 0.5H <sub>2</sub> O = 0.5Cu <sub>2</sub> O + H <sup>+</sup>	0.7	24 25	

**Figure 1.** (a)–(e) pH speciation diagrams for (a) 0.05 M Cu(II) and 1.5 M NH<sub>3</sub>, (b) 0.05 M Cu(I) and 1.5 M NH<sub>3</sub>, (c) 0.05 M Cu(II) and 0.5 M MEA (L = MEA, H<sub>1</sub>L = deprotonated MEA), (d) 0.05 M Cu(II) and 0.5 M TMDA, (e) 0.05 M Cu(II) and 0.1 M Tris, and (f) photographs of 0.05 M Cu(II) and 0.125 M MEA.



**Table III.** Weight change of the Cu<sub>2</sub>O on FTO substrate before and after immersion in aqueous solution containing 0.05 M CuSO<sub>4</sub> + 0.125 M MEA at pH 12.5 adjusted by NaOH, containing 0.05 M CuSO<sub>4</sub> + 0.1 M Tris at pH 12.5 adjusted by NaOH, containing 0.05 M CuSO<sub>4</sub> + 0.1 M TMDA at pH 7.4 adjusted by H<sub>2</sub>SO<sub>4</sub> or containing 0.05 M Cu(NO<sub>3</sub>)<sub>2</sub> + 0.05 M NH<sub>4</sub>NO<sub>3</sub> at pH 9 adjusted by NH<sub>3</sub>.

	MEA	Tris	TMDA	NH <sub>3</sub>
Before (net weight of Cu <sub>2</sub> O)	1.13 mg	1.13 mg	1.13 mg	1.13 mg
After (net weight of Cu <sub>2</sub> O)	1.12 mg	1.12 mg	1.10 mg	0.81 mg
Amount of change	0.01 mg	0.01 mg	0.03 mg	0.32 mg

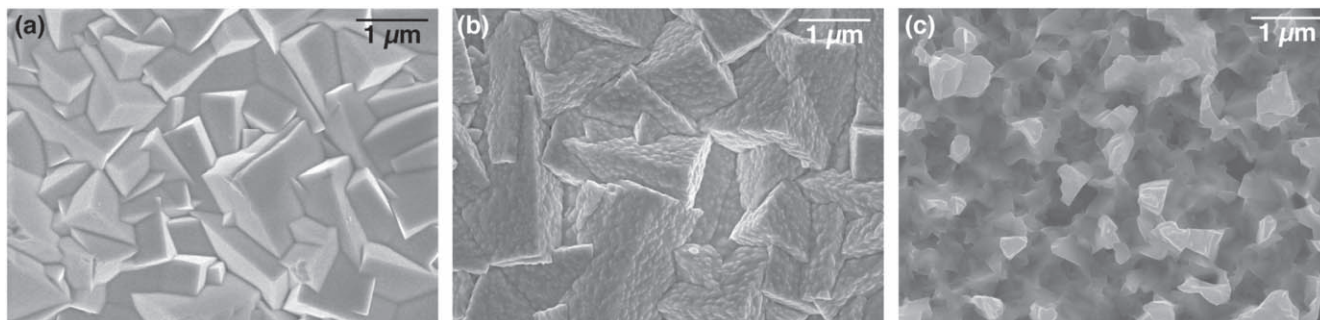


**Figure 2.** Top-view FE-SEM images of Cu<sub>2</sub>O (a) before immersion test and (b,c) after immersion test in MEA-based solution (b), and ammoniacal solution (c).

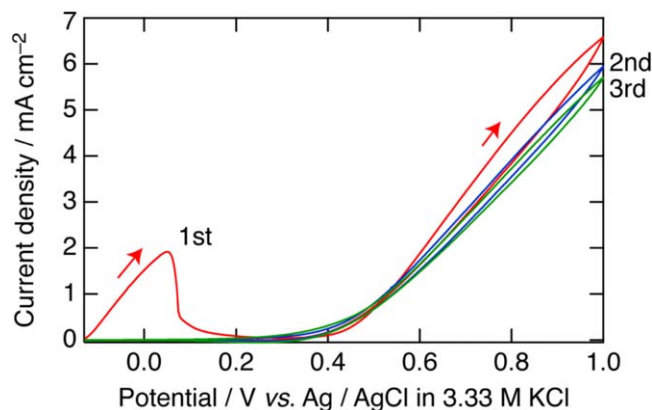
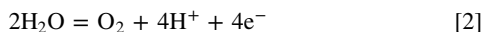
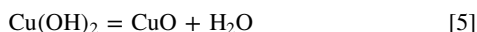
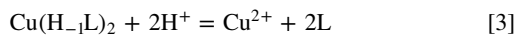


**Figure 3.** Cyclic voltammograms for the Cu<sub>2</sub>O-deposited FTO substrate in aqueous solution 0.05 M CuSO<sub>4</sub> + 0.125 M MEA solution at pH 12.5.



This oxygen evolution causes a local pH drop, which promotes the CuO electrodeposition (see Fig. 1c). The oxidation wave described by Eq. 1 was not observed during the second cycle or thereafter; CuO had already covered the anode surface due to the local pH drop as described by Eqs. 3, and 5, and thus, Cu<sub>2</sub>O hardly dissolved anodically.



As the result of CV, CuO is expected to precipitate at potentials more positive than that of the oxygen evolution reaction. In addition, since the oxidative dissolution reaction of Cu<sub>2</sub>O is suggested in Eq. 1, a reasonably fast deposition rate of CuO is necessary. Therefore, the potential was set at 0.45 V, which is a little more positive than the potential for oxygen evolution (approximately

0.4 V). Figure 4a shows XRD patterns of the layer obtained through potentiostatic deposition of CuO on the Cu<sub>2</sub>O/FTO layer. Together with the reflection due to cubic Cu<sub>2</sub>O, diffractions corresponding to monoclinic CuO were observed at 2θ of 35.6° and 38.5°. Figure 4b shows UV-vis absorbance spectra of Cu<sub>2</sub>O/FTO and CuO/Cu<sub>2</sub>O/FTO bilayers. The Cu<sub>2</sub>O/FTO layer has an absorption edge at 630 nm. In the case of the CuO/Cu<sub>2</sub>O bilayer, the absorption edge expanded to 900 nm, indicating that CuO acts as a light absorption layer. From this absorption edge, the band gap is estimated to be 1.38 eV, in good agreement with the previous reports on CuO.<sup>15</sup> As shown in Figs. 4c and 4e, the surface morphology changed after electrodeposition, and leaf-like crystals with the size of approximately 200–400 nm and the width of approximately 50 nm were observed. On the other hand, CuO crystals deposited on Au/Si from ammoniacal solution were reported to have fan-shaped grains with the size of approximately 100–150 nm and the width of approximately 15 nm.<sup>26</sup> It is generally known that ligands affect the morphology of the electrodeposits by adsorbing on the surface.<sup>27,28</sup> The leaf-like morphology in Fig. 4e might be due to such effect. However, it is known that crystal morphology is affected also by the underlying layer. Because of the difference in underlying layer, i. e. Cu<sub>2</sub>O or Au/Si, the effect of the MEA on the crystal shape is not clear at this time. The cross-sectional images in Figs. 4d and 4f show a bilayered structure, with no significant changes from the cross section of the Cu<sub>2</sub>O-deposited FTO substrate. Therefore, the Cu<sub>2</sub>O base layer was not dissolved, and the layering of CuO on Cu<sub>2</sub>O was successful. Since the CuO precipitation took place fast enough, the anodic dissolution of Cu<sub>2</sub>O corresponding to Eq. 1 was minimized. The anodic dissolution of Cu<sub>2</sub>O (Eq. 1) is expected to be affected by the potential applied, and the effect will be clarified in the future.

XPS spectra for the CuO surface deposited on Cu<sub>2</sub>O were obtained. Figure 5 shows the high-resolution spectrum of the layer. The Cu2p<sub>1/2</sub> and Cu2p<sub>3/2</sub> peaks at 954 and 936 eV confirmed the presence of CuO. In addition, a few carbonate-derived peaks were found in the C 1s spectra at 285 and 289 eV, while no other impurities such as MEA-derived nitrogen or sulfate-derived sulfur were detected. Moreover, the quantitative analyses showed that the layer surface contained 47.8 at.% Cu, 45.6 at.% O, and 6.6 at.% C, with no other elements. These results indicate that nearly-pure CuO was deposited.

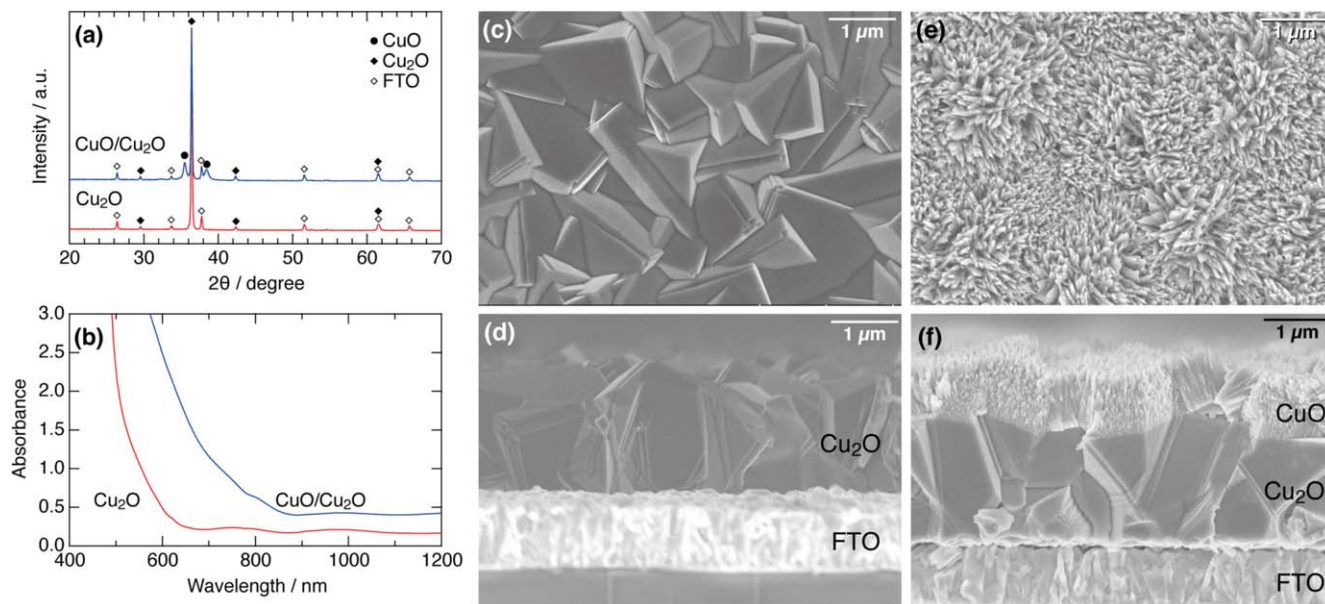


**Figure 4.** (a) XRD profiles and (b) Vis-NIR absorbance spectra of the  $\text{Cu}_2\text{O}$  and  $\text{CuO}/\text{Cu}_2\text{O}$  layers prepared on FTO, and (c), (e) Top-view, and (d), (f) cross-section-view FE-SEM images of the  $\text{Cu}_2\text{O}$  (c), (d) and  $\text{CuO}/\text{Cu}_2\text{O}$  (e), (f) layers prepared on FTO.

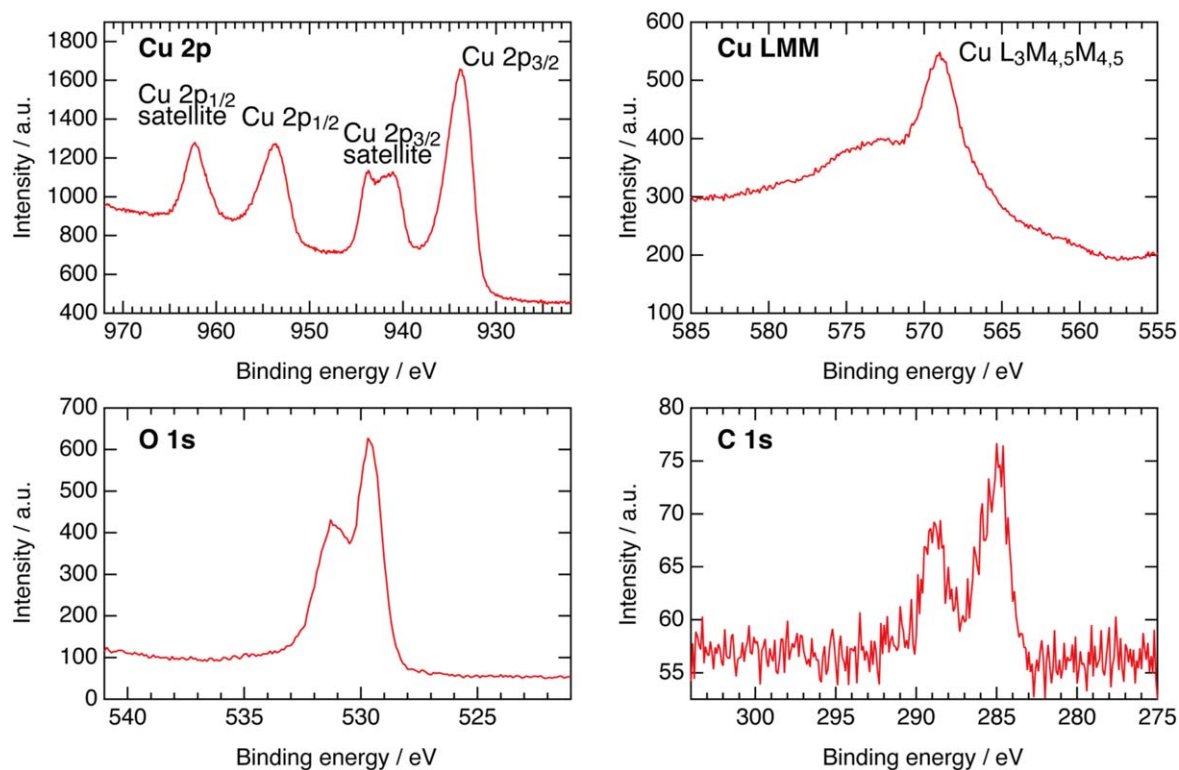
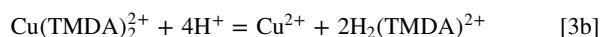
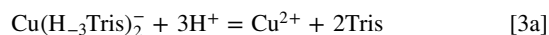
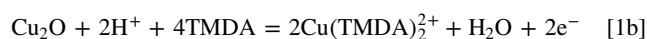
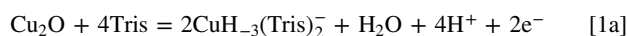


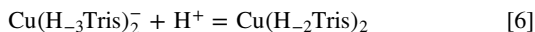
**Figure 5.** XPS Cu 2p, Cu LMM, O 1s, C1s spectra of the CuO surface of the  $\text{CuO}/\text{Cu}_2\text{O}$  bilayer.

***CuO electrodeposition on  $\text{Cu}_2\text{O}$  using Tris and TMDA based solutions.***—Figure S2 shows cyclic voltammograms for the  $\text{Cu}_2\text{O}/\text{FTO}$  layer in the Tris and TMDA solution. As in the case of MEA solution, the oxidation waves corresponding to Eqs. 1a, 1b were observed only in the 1st cycle. These indicate that CuO covered the  $\text{Cu}_2\text{O}$  surface by a series of reactions 3a, 4, and 5 or 3b, 4, and 5.



XRD patterns of anodic CuO electrodeposited from Tris or TMDA solutions on  $\text{Cu}_2\text{O}/\text{FTO}$  gave a set of diffraction peaks of  $\text{Cu}_2\text{O}$  and CuO (Fig. S3). CuO electrodeposited from the TMDA solution showed columnar crystals with a size of approximately 300–400 nm, and thickness of CuO layer was approximately 1  $\mu\text{m}$  (Figs. S4a and S4c). In

contrast, CuO electrodeposited from the Tris solution showed crystals with a size of about 100 nm and a width of about 10 nm, and thickness of CuO layer was approximately 250 nm (Fig. S4b and Fig S4d). The thickness of CuO electrodeposited from Tris solution was smaller than that of TMDA solution probably due to the concomitance of reaction 6 in addition to the reactions 3', 4, and 5 by the pH decrease through the oxygen evolution.



From the cross-sectional images (Figs. S4b and S4d), it can be seen that there are two layers. Together with the results of XRD, it can be concluded that the upper layer is CuO. As in the case of MEA, CuO was successfully stacked on Cu<sub>2</sub>O using Tris and TMDA-based solution.

**CuO electrodeposition on Cu<sub>2</sub>O using conventional ammoniacal solution.**—Figure S5 shows an XRD pattern and Fig. S6 shows surface and cross-sectional FE-SEM images of the sample prepared by anodic CuO electrodeposition on Cu<sub>2</sub>O under the conditions reported in the literature.<sup>15</sup> The diffraction peaks of CuO were observed together with Cu<sub>2</sub>O, but the diffraction peaks of Cu<sub>2</sub>(NO<sub>3</sub>)(OH)<sub>3</sub> were also observed. The cross-sectional FE-SEM image shown in Fig. S6d shows a three-layered structure with layers above and below the Cu<sub>2</sub>O. From XRD, both of the layers above and below the Cu<sub>2</sub>O are mixed layers of CuO and Cu<sub>2</sub>(NO<sub>3</sub>)(OH)<sub>3</sub>. We expected that increasing the solution temperature would accelerate the hydrolysis reaction and stimulate the deposition of pure CuO. However, as the temperature increased, more precipitates that appeared to be hydroxides, were generated from the ammoniacal solution. So, the solution composition is not suitable for increasing the temperature. In addition, the film's overall adhesion deteriorated in the ammoniacal solution, and a partial peeling off from the substrate and a number of cracks were observed (Fig. S6a, S6b). The peeling off and cracks may well be attributed to the reaction of ammonia with Cu<sub>2</sub>O. As a result, CuO and Cu<sub>2</sub>(NO<sub>3</sub>)(OH)<sub>3</sub> were precipitated on both sides of Cu<sub>2</sub>O layer. If the rate of CuO coverage is fast enough, the effect of ammonia reacting with Cu<sub>2</sub>O can be minimized. However, the conditions of the CuO deposition method using this ammoniacal solution were not sufficient.

**General discussion.**—This solution design resulted in successful stacking of an upper layer (CuO) by electrodeposition without dissolving the base layer (Cu<sub>2</sub>O). Despite the dissolution peak in CV, CuO electrodeposition proceeded without dissolving Cu<sub>2</sub>O. This is probably due to the rate of CuO (Cu(OH)<sub>2</sub>) formation due to the local pH drop being faster than the electrochemical dissolution rate of Cu<sub>2</sub>O. The effect of CuO electrodeposition and conditions such as applied potential, solution composition and temperature on the base layer performance will be clarified in future studies.

## Conclusions

As an example rational solution design for electrodeposition of multilayered semiconductors, we focused on a CuO/Cu<sub>2</sub>O bilayer. Our approach was to identify, using a thermodynamic database, suitable ligands for CuO electrodeposition that keep Cu<sub>2</sub>O insoluble. MEA, Tris, and TMDA were identified as appropriate candidate ligands, while the frequently-used ammonia was found to dissolve Cu<sub>2</sub>O. The MEA, Tris and TMDA-based CuO electrodeposition solution did not dissolve Cu<sub>2</sub>O. Anodic CuO electrodeposition on Cu<sub>2</sub>O from each of the three ligands in aqueous solutions was

successfully achieved. The CuO/Cu<sub>2</sub>O bilayer is attractive as a photocathode for water splitting, and it will be interesting to evaluate its photovoltaic performance in future studies. The rational design of electrodeposition solutions for multilayered materials is important, because dissolution of lower layers is sensitive to various properties. Our method should be applicable not only to other multilayer semiconductors, but also to bilayer of metals and alloys.

## Acknowledgments

The authors acknowledge Mr. Yutaka Sonobayashi (Kyoto University) for supporting the XPS measurements. This work was supported financially by Grants-in-Aid for Grants-in-Aid for Scientific Research (S) (No. 20H05663: K. M.) from the Japan Society for the Promotion of Science. This work was partly supported by Kyoto University Nano Technology Hub in "Nanotechnology Platform Project" sponsored by the Ministry of Education, Culture, Sports, Science and Technology (MEXT), Japan.

## ORCID

Atsushi Kitada  <https://orcid.org/0000-0002-4387-8687>  
Kazuhiro Fukami  <https://orcid.org/0000-0001-9120-5578>  
Kuniaki Murase  <https://orcid.org/0000-0002-7564-9416>

## References

- H. Ohta, M. Hirano, K. Nakahara, H. Maruta, T. Tanabe, M. Kamiya, T. Kamiya, and H. Hosono, *Appl. Phys. Lett.*, **83**, 1029 (2003).
- I. S. Jeong, J. H. Kim, and S. Im, *Appl. Phys. Lett.*, **83**, 2946 (2003).
- Y. Hirai, Y. Kurokawa, and A. Yamada, *Jpn. J. Appl. Phys.*, **53**, 012301 (2014).
- F. Lang et al., *Joule*, **4**, 1054 (2020).
- A. Paracchino, V. Laporte, K. Sivula, M. Grätzel, and E. Thimsen, *Nat. Mater.*, **10**, 456 (2011).
- H. Kumagai, T. Minegishi, N. Sato, T. Yamada, J. Kubota, and K. Domen, *J. Mater. Chem. A*, **3**, 8300 (2015).
- W. Zhang et al., *Sci. Rep.*, **4**, 3826 (2014).
- J. Li, H. Wang, M. Luo, J. Tang, C. Chen, W. Liu, F. Liu, Y. Sun, J. Han, and Y. Zhang, *Sol. Energy Mater. Sol. Cells*, **149**, 242 (2016).
- J. Su, L. Guo, N. Bao, and C. A. Grimes, *Nano Lett.*, **11**, 1928 (2011).
- S. A. Mansour and F. Yakuphanoglu, *Solid State Sci.*, **14**, 121 (2012).
- K. Fujimoto, T. Oku, and T. Akiyama, *Appl. Phys. Express*, **6**, 086503 (2013).
- M. R. Shaner, K. T. Fountaine, S. Ardo, R. H. Coridan, H. A. Atwater, and N. S. Lewis, *Energy Environ. Sci.*, **7**, 779 (2014).
- S. Ho-Kimura, S. J. A. Moniz, J. Tang, and I. P. Parkin, *ACS Sustain. Chem. Eng.*, **3**, 710 (2015).
- Y. Yang, D. Xu, Q. Wu, and P. Diao, *Sci. Rep.*, **6**, 35158 (2016).
- M. Izaki, M. Nagai, K. Maeda, F. B. Mohamad, K. Motomura, J. Sasano, T. Shinagawa, and S. Watase, *J. Electrochem. Soc.*, **158**, D578 (2011).
- R. M. Smith and A. E. Martell, *Critical Stability Constants, Amino Acids* (Plenum Press, New York, NY) **2** (1975).
- R. Tauler, E. Casassas, and B. M. Rode, *Inorganica Chim. Acta*, **114**, 203 (1986).
- J. Nagaj, K. Stokowa-Sołtys, E. Kurowska, T. Frączyk, M. Jeżowska-Bojczuk, and W. Bal, *Inorg. Chem.*, **52**, 13927 (2013).
- A. E. Rakhshani, A. A. Al-Jassar, and J. Varghese, *Thin Solid Films*, **148**, 191 (1987).
- T. D. Golden, M. G. Shumsky, Y. Zhou, R. A. VanderWerf, R. A. Van Leeuwen, and J. A. Switzer, *Chem. Mater.*, **8**, 2499 (1996).
- K. Mizuno, M. Izaki, K. Murase, T. Shinagawa, M. Chigane, M. Inaba, A. Tasaka, and Y. Awakura, *J. Electrochem. Soc.*, **152**, C179 (2005).
- R. M. Smith and A. E. Martell, *Critical Stability Constants, Inorganic Complexes* (Plenum Press, New York, NY) **4**, 41 (1976).
- R. M. Smith and A. E. Martell, *Critical Stability Constants, Amines* (Plenum Press, New York, NY) **2**, 51 (1975).
- R. M. Smith and A. E. Martell, *Critical Stability Constants, Inorganic Complexes* (Plenum Press, New York, NY) **4**, 6 (1976).
- R. M. Smith and A. E. Martell, *Critical Stability Constants, Inorganic Complexes* (Plenum Press, New York, NY) **4**, 8 (1976).
- P. L. Khoo, M. Nagai, M. Watanabe, and M. Izaki, *J. Surf. Finish. Soc. Jpn.*, **69**, 469 (2018).
- L. Xu, Y. Guo, Q. Liao, J. Zhang, and D. Xu, *J. Phys. Chem. B*, **109**, 13519 (2005).
- M. A. Pasquale, L. M. Gassa, and A. J. Arvia, *Electrochim. Acta*, **53**, 5891 (2008).